Atmos. Chem. Phys. Discuss., 4, 2569–2613, 2004
www.atmos-chem-phys.org/acpd/4/2569/
SRef-ID: 1680-7375/acpd/2004-4-2569

Atmospheric Chemistry and Physics Discussions

Using GOME NO_2 satellite data to examine regional differences in TOMCAT model performance

N. H. Savage[1], K. S. Law[1,*], J. A. Pyle[1], A. Richter[2], H. Nüß[2], and J. P. Burrows[2]

[1]Centre for Atmospheric Science, Chemistry Department, University of Cambridge, UK
[2]Institute of Environmental Physics, University of Bremen, NW1, Kufsteiner Strasse 1, D-28359 Bremen, Germany
[*]Now at: Service d'Aeronomie, CNRS/IPSL, Paris, France

Received: 26 February 2004 – Accepted: 18 March 2004 – Published: 12 May 2004

Correspondence to: N. H. Savage (nick.savage@atm.ch.cam.ac.uk)

Abstract

This paper compares column measurements of NO_2 made by the GOME instrument on ERS-2 to model results from the TOMCAT global CTM. The overall correlation between the model and observations is good (0.79 for the whole world, and 0.89 for north America) but the modelled columns are too large over polluted areas (gradient of 1.4 for North America and 1.9 for Europe). NO_2 columns in the region of outflow from North America into the Atlantic seem too high in winter in the model compared to the GOME results, whereas the modelled columns are too small off the coast of Africa where there appear to be biomass burning plumes in the satellite data. Several hypotheses are presented to explain these discrepancies. Weaknesses in the model treatment of vertical mixing and chemistry appear to be the most likely explanations. It is shown that GOME and other satellite data will be of great value in furthering our understanding of atmospheric chemistry and in targeting and testing future model development and case studies.

1. Introduction

Nitrogen dioxide (NO_2) plays a central role in tropospheric chemistry. NO_2 photolysis is the major tropospheric source of ozone; NO_2 is recycled in a catalytic manner via reactions with peroxy radicals (Haagen-Smit, 1952). In many regions of the atmosphere ozone production is NO_x–limited (e.g. Chameides et al., 1992). Therefore a correct simulation of the budget of NO_x (NO_2+NO) is a prerequisite for an accurate model ozone budget. The Intergovernmental Panel on Climate Change Third Assessment Report (IPCC-TAR, Houghton et al., 2001) gives an estimate of a global average radiative forcing of $+0.35\pm0.15\,W\,m^{-2}$ due to increases in tropospheric ozone since pre-industrial times making it the third most important greenhouse gas after CO_2 and CH_4. They also assigned this forcing a medium level of scientific understanding and highlighted how model-model differences affected calculated ozone budgets. Under-

ACPD

4, 2569–2613, 2004

standing the contribution of NO_x is clearly essential. In addition to its role in the ozone budget, nitrogen dioxide is also oxidised to form nitric acid which plays an important role in acidification and can also act as a nutrient with important impacts on ecosystems (e.g. Borrell et al., 1997).

Model validation studies using a variety of data sets have shown that models find the simulation of the NO_y budget to be a challenge. For example Grewe et al. (2001) found that two coupled chemistry climate models were unable to reproduce the gradient in NO_x mixing ratio between North America and the Atlantic Ocean and had problems correctly reproducing vertical gradients. Thakur et al. (1999) found that models tended to under-predict global free tropospheric NO while over-predicting HNO_3 and PAN. Brunner et al. (2003) found that results for NO_x differed quite significantly between models. Specific problems included the inability to model locally elevated NO_x in plumes. For many field campaigns models underpredicted NO_x especially in regions recently impacted by lightning.

A major part of the challenge in improving model performance is the large number of different processes which have an impact on chemical concentrations and distributions. If the total emissions of one or more chemical compounds are incorrect, or if these emissions are not distributed correctly across the world, the model will be unable to predict the concentrations of short lived species accurately. As most emissions occur close to the ground, dry deposition and boundary layer mixing have a strong impact on the total burden of many species. The model then needs to simulate the large scale advection of the chemical species. Convection and other processes such as frontal uplifting of air masses not only redistribute species vertically but as the wind speeds increase with height has a substantial impact on the horizontal distribution. In addition, the lifetime and subsequent chemistry of NO_x is also a function of height. Uplifted air masses are cooler which favours the formation of PAN, a key reservoir of NO_x. The photolysis of nitric acid is also more rapid at higher levels and so is more likely to regenerate NO_x unless it is removed by washout. These and many other changes in the chemical environment with height imply that the lifetime and distribution of NO_2 will

be strongly influenced by the speed and extent of vertical transport. The rate of ozone production is also affected due to its non-linear dependence on NO_x concentration (e.g. Sillman et al., 1990).

Finally, in order to correctly model the distribution and concentration of any species, the chemical reactions in which it is involved must be adequately modelled. So, errors in model results for any particular species may be due not to model problems in emissions and physical processes affecting the species of interest but may result from problems in modelling other related compounds. For example, if the modelled concentrations of methane are too high this might reduce OH concentrations thus reducing the lifetime of NO_x.

With this degree of interaction and complexity in the atmospheric chemistry system, the physical and chemical processes occurring in the atmosphere have to be simplified in models. The broader the range of measurements used to validate models the better. Long term measurements at ground stations have the advantage of giving a long time series but have restricted spatial coverage. Aircraft measurements have been invaluable to further our understanding but offer only limited spatial and temporal coverage (see for example Thakur et al., 1999). Satellite measurements offer the advantage of making measurements which are both global and long term.

Several recent studies have used a combination of GOME satellite measurements with global models to assess both the consistency of the GOME data and validate models. Velders et al. (2001) compared monthly average NO_2 columns from the global CTMs IMAGES and MOZART to GOME measurements for 1997. They found that the columns over Europe and North America were of the same order as those calculated by the MOZART model but were a factor of 2–3 higher over Asia. Lauer et al. (2002) compared a climatological data set for NO_2 to the first 5 years of the GOME measurements. They examined the seasonal evolution of the column over Europe, the Eastern USA, Africa, South America, Australia and Southeast Asia. They found an overestimation by the GCM of 2 to 3 times. Kunhikrishnan et al. (2003) compared the results of the MATCH-MPIC model from 1997 and 1998, with a focus on the seasonal columns

over various parts of the Asian region. They found that seasonal average NO_2 columns from the model were comparable to the satellite results but there were problems with the seasonal cycle over India. Martin et al. (2002) calculated correlation coefficients between GOME and GEOS-CHEM calculations for the USA and the whole world using data from July 1996. For the USA the GOME results were within 18% of the model results and had a correlation coefficient of 0.78.

In this paper the previous analyses are extended by combining the methods of correlation studies and the use of comparisons of seasonal columns, using a wider range of regions and examining an entire year's output from a CTM. The results are compared to those of previous studies. We aim to show how GOME NO_2 column measurements can be used to highlight areas of disagreement as a means to target and test future model development and develop validation strategies. Identifying areas of disagreement between the model and satellite measurements can give insight into which model processes require development as well as identifying regions of the world where especially important and/or interesting events are taking place. This will further our understanding of the atmospheric chemistry system as a whole.

Section 2 discusses how NO_2 columns were retrieved from the GOME data and Sect. 3 describes TOMCAT, the chemistry-transport model used for this study. The model results are compared to the GOME retrievals in Sect. 4 and reasons for differences are examined in Sect. 5.

2. Satellite data

GOME is a spectrometer on board ERS-2. It was launched on 20 April 1995 and flies in a sun-synchronous, polar orbit at an average height of 785 km above the Earth's surface (Burrows et al., 1999, and references therein). The GOME instrument observes in nadir viewing geometry the light (UV/visible) scattered back from the atmosphere and reflected at the ground. Once per day, it also observes the extraterrestrial solar irradiance. The instrument is designed to observe simultaneously the spectral

ACPD
4, 2569–2613, 2004

range between 232 and 793 nm. The atmosphere is scanned with a spatial resolution of 320 km×40 km (across track×along track) (forward scan) and 960 km×40 km (back scan). Each individual orbit of ERS-2 takes about 100 min. Although the repeating cycle of an orbit is 35 days, nearly global coverage (except for a small gap around the poles) is achieved within three days applying the maximum scan width of 960 km (ESA, 1995). As a result of the sun-synchronous orbit, the measurements in low and middle latitudes are always taken at the same local time (LT) with, for example, the northern mid-latitudes being crossed at about 10:45 LT.

The trace gas retrieval of NO_2 is achieved using the DOAS technique (Differential Optical Absorption Spectroscopy). This technique utilises the atmospheric absorption, defined as the natural logarithm of the ratio of the extraterrestrial irradiance and the earth-shine radiance, for a selected spectral window. This is compared with reference absorption spectra of gases absorbing in the spectral window and a polynomial of low order. The polynomial describes the scattering and broad absorption in the window. The slant column of a gas is derived from the differential absorption of the gas in question and to a first approximation is the integrated concentration along the light paths through the atmosphere. For this study, the spectral window from 425 to 450 nm has been used, the spectra of NO_2, O_3, O_4 and H_2O and a reference Ring spectrum being fitted (Richter and Burrows, 2001).

The resultant slant columns of NO_2 include both the stratospheric and the tropospheric signal. To isolate the tropospheric column, a modified reference sector or tropospheric excess method (TEM) was applied. Originally, in this method measurements taken over the Pacific Ocean were subtracted from all other measurements assuming that this region has negligible tropospheric NO_2 columns and that the stratosphere is zonally invariant with respect to NO_2 (Richter and Burrows, 2001). Here, the stratospheric zonal variability was explicitly taken into account by using daily stratospheric NO_2 fields from the 3D-CTM SLIMCAT (Chipperfield, 1999). To account for differences between the stratospheric columns as measured by GOME and those modelled by SLIMCAT, the model results were normalised to the values in the reference sector.

With this correction, the consistency of the GOME NO_2 columns was much improved in particular at Northern mid and high latitudes in spring. It has to be pointed out that as a result of the normalisation the values still represent a tropospheric excess which does not account for the residual tropospheric NO_2 column in the reference region.

The tropospheric slant columns are converted to vertical columns by the application of an air mass factor, AMF. The AMF describes the effective length of the light path through the atmosphere relative to a vertical transect and is derived from radiative transfer calculations. The value of the AMF depends on the viewing geometry and the solar zenith angle, but also on surface albedo, vertical gas profile, clouds and atmospheric aerosol. In this study, the AMFs used have been improved compared to the ones described in Richter and Burrows (2001) in several respects. The value used for surface albedo is taken from the monthly climatology of Koelemeijer et al. (2001) which is based on GOME measurements; surface elevation is accounted for and extinction by aerosol is treated using three different scenarios (maritime, rural and urban) which were selected based on the geographical location. Most importantly, the vertical profile of NO_2 used is taken from the daily results of the TOMCAT model run for 1997 described below. This implies that the comparisons shown are self consistent, in particular for transport events where vertical displacement changes the sensitivity of GOME to the NO_2. This greatly reduces the uncertainty in the comparison as discussed in Eskes and Boersma (2003). The impact of this on the model-data comparison is discussed later. Stratospheric NO_2 is not included in the airmass factor calculation as the tropospheric slant columns have already been corrected for the stratospheric contribution as explained above, and the influence of stratospheric NO_2 on the radiative transfer can be neglected (Richter and Burrows, 2001; Velders et al., 2001). More details of retrieval methods and a full error analysis can be found in Richter and Burrows (2001).

For this study, climatological monthly means of the tropospheric NO_2 column amounts (January 1997 to December 1997) have been used. The data were selected to be cloud free, i.e. only pixels having a cloud coverage below a threshold value of 10% were used to derive the tropospheric NO_2 column amounts from the GOME mea-

surements.

3. TOMCAT global model

3.1. TOMCAT model description

TOMCAT is a global three dimensional chemistry-transport model (CTM). Meteorological analyses from the European Centre for Medium Range Weather Forecasting (ECMWF) are used as input to the model for winds, temperatures and humidity. Tracer transport is calculated using the Prather advection scheme (Prather, 1986) with a 30 min dynamical time-step. Moist convective transport of tracers is performed using a mass flux scheme (Tiedtke, 1989) and a non-local vertical mixing scheme is used based on that developed for the NCAR Community Climate Models, Version 2 (Holtslag and Boville, 1993). The chemistry is integrated using the ASAD chemistry package (Carver et al., 1997). There is no heterogenous loss of N_2O_5 on aerosol in the model at present. However the reaction of N_2O_5 with gas phase water vapour is included. The version of the model used here has 31 vertical levels and a horizontal resolution of approximately 2.8×2.8° from the ground up to 10 hPa and has a total of 39 chemical species of which 30 are advected. The TOMCAT model was run with a 4 month spin up from September 1996. Model results for the whole of 1997 were used to compare to GOME data.

The emissions data set used here is the same as that used for the POET model intercomparison study (Savage et al., 2003). The anthropogenic emissions are based on Edgar 3 (Olivier et al., 2001) modified to be appropriate for 1997 as described in Olivier et al. (2003). Biomass burning emissions however are based on climatological values and so are not specific to 1997. This is particularly significant as 1997 saw unusual biomass burning emissions due to the effect of the strong El Niño in that year. For more details of the model intercomparison see Savage et al. (2003). Lightning emissions in the model are scaled to a global annual total of 5 Tg(N) per year.

ACPD
4, 2569–2613, 2004

3.2. Radon tracer experiment

Radon is a chemically inert tracer which undergoes radioactive decay with a lifetime of 5.5 days. Its major emission sources are over land and it has been used previously in model intercomparison studies to examine model transport properties (see for example Jacob et al., 1997; Rasch et al., 2000). As part of the POET intercomparison study (Savage et al., 2003) the TOMCAT model performed the radon experiment described in Jacob et al. (1997) for the year 1997 allowing transport processes in the model to be assessed. The results are useful as a means of separating physical and chemical influences on the NO_2 distribution. Some results will be discussed in Sect. 5.3.1

3.3. Model data processing

In order that the model and satellite data are truly comparable some care has been taken in processing the model results. There are two main issues to be addressed. Firstly the ERS-2 satellite is in a sun synchronous orbit and has an equator crossing time of 10:30. Standard TOMCAT model output is at 0:00, 06:00, 12:00 and 18:00 GMT so the local time of output varies as a function of longitude. In order to remove this effect the model was modified to output data every time-step for those grid points where the local time was close to 10:30 in addition to standard model output. The second issue concerns the separation of the tropospheric and stratospheric columns. Although TOMCAT is a tropospheric model the top levels extend into the stratosphere and so removal of this component is necessary. To make this as close as possible to the TEM method used for the satellite data, as outlined above, the following procedure was used: first the column up to the 350 K isentropic level (the bottom level of the SLIMCAT data used for tropospheric removal) was calculated and then a clean sector average was subtracted. This is referred to as the "best" method.

In order to evaluate the importance of the methods used to determine the modelled tropospheric columns two other methods of calculating the column were used. In the first of these a monthly mean of the standard model 6 hourly output files was calculated

ACPD
4, 2569–2613, 2004

to give a 24 h average.

The same tropospheric subtraction as outlined above was then applied (referred to as "Standard Output"). The second test used the 10:30 columns but calculated the column up to the thermal tropopause as defined by the WMO (WMO, 1957). This is referred to as the "WMO" method. The correlation of these different model data sets with GOME columns were then calculated. To compare GOME data directly with the much lower resolution TOMCAT results, monthly mean satellite data were averaged onto the same grid as the model before performing any correlations. The linear regressions were found using the ordinary Least Squares Bisector calculated by the IDL routine "sixlin" obtained from the IDL Astronomy Library http://idlastro.gsfc.nasa.gov/homepage.html (Landsman, 1993). The ordinary least squares bisector is an appropriate regression method when the intrinsic scatter in the data dominates any errors arising from the measurement process – see Isobe et al. (1990). The linear Pearson correlation coefficient was also calculated using IDL.

Table 1 shows the mean results of these correlations. If values from the standard model output are used instead of the 10:30 local output there is a significant increase in the gradient of the correlation. This is to be expected as a 24 h average will include many points at night where the NO_2/NO_x ratio is almost 1. The results are not so sensitive to the method used to calculate the model tropospheric column, although there is a small decrease in the correlation coefficient when the WMO definition of the tropopause was used. This is in agreement with Martin et al. (2002) who found only a very small increase in correlation coefficient when they corrected their data for Pacific sector bias. For July 1997 they found a correlation coefficient of 0.76 for the whole world which is very close to the annual average value of 0.79 found here. All further comparisons with the GOME data use TOMCAT results output at 10:30 local time with the stratospheric subtraction.

ACPD
4, 2569–2613, 2004

4. Results

In this section the model results are compared to the GOME data. The extent to which model results and GOME data agree has been examined by focusing on four points: the global distribution of NO_2; correlations between the two data sets on a region by region basis; the export of NO_2 from polluted regions and NO_2 columns over biomass burning areas. In Sect. 5 possible explanations for differences between the model and measurements are then discussed in a process-orientated manner.

4.1. Global distribution of NO_2

Figures 1, 2 and 3 show January, July and September 1997 monthly mean column amounts of NO_2 calculated from GOME satellite measurements and TOMCAT. In contrast to the correlation studies mentioned previously these figures show the GOME columns at $0.5 \times 0.5^{\circ}$ resolution. For these months the overall agreement between the satellite measurements and the model is reasonably good. According to the Edgar 3.2 emissions inventory (Olivier et al., 2001) for 1995, 22% of all anthropogenic NO_x emissions were from the USA and Canada, with 13% from OECD Europe and 25% from Asia. These areas with high anthropogenic NO_x emissions can be seen as areas of high total column density in both the GOME data and the model results. The total column amounts are in good agreement for January although for July, especially over Europe, the modelled columns are greater than the GOME data. Both the model and the GOME measurements show that the highest columns are found over northern Europe in the area of southern England, the Benelux countries and Germany. However the high concentrations over northern Italy seen by GOME in January are not resolved by the model as its spatial resolution is too low.

In contrast Velders et al. (2001) found that the modelled columns from the MOZART model were much higher than the measured values in January for Europe and agreed better with the GOME measurements over Europe for July. Lauer et al. (2002) tend to overestimate the European columns in both January and July which they attribute to the

ACPD
4, 2569–2613, 2004

absence of a sink for N_2O_5 on aerosol in their model. Martin et al. (2002) have better agreement than TOMCAT for July but in contrast to the TOMCAT model underestimate the columns over Europe. It must be noted however that all these studies used different retrievals of GOME NO_2 as well as different models.

In Asia both TOMCAT and GOME have the highest columns over Japan and in China in the region around Beijing. Elevated columns are also seen over the Indian subcontinent. The highest columns over North America are on the East coast with some smaller peaks over the West Coast in the region around Seattle. The main region of biomass burning over West Africa in January can also be seen in both the model and the GOME data. The seasonality of biomass burning emissions in the model follows closely that observed by the satellite data, with a southward movement of the areas of burning through the year due to the seasonality in the position of the ITCZ as has been documented previously e.g. Hao and Liu (1994). In the region near the west coast of Africa from the equator to about 20° south (described as central Africa in this paper) elevated NO_2 from biomass burning can be clearly seen in July in both the model and the GOME data (see Fig. 2).

The biomass burning regions and their seasonal patterns are seen in the previous studies as well. This seasonality is examined further in Sect. 4.4.

Downwind of both North America and south-east Asia are regions where there are columns which are greater than the background concentrations. This is clearest in January but can also be seen in July and September to a certain extent. This indicates export of NO_x from these areas, however it should be noted that some of the NO_2 in the North Atlantic also comes from aircraft and ship emissions. There are also elevated columns of NO_2 off the west coast of Africa in the satellite data. This agrees qualitatively with measurements of Biomass Burning emissions blowing off West Africa into the ocean – see, for example, Harris et. al (1992) and Burkert et. al (2001). These possible outflow regions are considered in more detail in Sect. 4.3.

ACPD
4, 2569–2613, 2004

4.2. Correlations of TOMCAT results with GOME data

To examine in a more quantitative manner how well the model agrees with measurements for regions of high NO_2 columns correlations were calculated on a region by region basis. These regions were defined as shown in Table 2. The same methods were used to calculate regressions and correlation coefficients as for the global correlations described previously (Sect. 3.3)

Tables 3 and 4 show the Pearson correlation coefficient and the gradient and intercept for all months for the regions where correlations were calculated. There are good correlations over polluted areas with mean values ranging from 0.71 for Asia to 0.89 for north America. The reason why the agreement is better for more polluted regions may be that the emissions inventories for anthropogenic emissions are more accurate because it is easier to estimate the regions of greatest emission and spatial extent for anthropogenic emissions than for biomass burning and natural emissions. In the polluted regions the intercept for most months is small but the gradients vary widely. Martin et al. (2002) found a correlation coefficient of 0.78 for the USA in July 1997 which is somewhat lower than the value obtained here for North America of 0.93.

The range of gradients during 1997 is the greatest over Europe. The gradient is greater than 1 for all months except January and there is a distinct seasonal cycle in the gradients. In the winter months the model is closest to a 1:1 correlation with the GOME data while the largest gradient (3.14) is calculated in June. Figure 4 shows a scatter plot of modelled columns versus GOME retrievals over Europe. It can be seen that the majority of points lie well above the 1:1 line and the model fails to correctly predict the GOME columns. Further evidence for this strong seasonal difference is found when the mean column over Europe is calculated from the TOMCAT data and using the GOME data re-gridded onto the TOMCAT model grid (Fig. 5). The error bars are the standard deviation of the column over this area.

On average over Europe the mean TOMCAT column is between 1.1 and 2.7 times higher than GOME. This difference is the highest in the late spring and early summer

ACPD
4, 2569–2613, 2004

months. The seasonal cycle in TOMCAT is qualitatively correct though with a minimum in the summer months. The model has a larger standard deviation than the measurements in the summer, while in January when the TOMCAT measurements are the closest to the GOME data, the standard deviation is smaller. This is similar to the results of Lauer et al. (2002) for Europe, however the overestimate of this column is much less pronounced than in that study. However that study used a GCM with only a preliminary tropospheric NO_x chemistry.

A similar but less pronounced pattern is seen for Asia and North America. Both have only one month where the gradient of the correlation is less than 1. The highest correlations in both are also in the summer months (August for North America, May for Asia). However the maximum gradients are much lower – 1.74 for North America and 1.86 for Asia. Kunhikrishnan et al. (2003) found that model-GOME agreement was not consistent in all Asian sub-domains with India having the worst agreement and the model failing to capture the biomass burning peaks for North Asia and China. If smaller sub-domains were used it might improve the agreement for some areas.

Over Africa a completely different pattern emerges. The minimum value of the gradient is in April (0.68) and the maximum (1.77) is in November. During the 2 major biomass burning seasons, the concentrations calculated by the model are greater than those seen by GOME. This can also be seen in the plots of January and July where the columns in the regions of high concentrations are greater in the model than in the satellite data (see Figs. 1 and 2). African biomass burning is investigated in more detail in Sect. 4.4.

The oceanic regions have much lower correlations and gradients which are very small compared to those over source regions. The lower correlations might be expected as the range of values is smaller and thus the impact of errors will be greater. There is also a major difference between the North and South Atlantic. As well as having a smaller correlation, the North Atlantic has a higher mean gradient (despite 2 months where it has a large negative gradient).

Figures 6 and 7 show a scatter plot of TOMCAT versus GOME for the North and

ACPD
4, 2569–2613, 2004

South Atlantic respectively. These figures show why there is such a difference in the correlations and gradients in the two regions. The South Atlantic (Fig. 6) has a single population of data with all modelled values low and most below the 1:1 line. It would appear that in this region which is remote from most anthropogenic influence the modelled concentrations are much too low. We can see these lower concentrations in the plots of the global data also. In contrast, there seem to be two distinct populations in the North Atlantic (Fig. 6), one of low values similar to the South Atlantic and a second which is much higher. This is due to either outflow from North America or the influence of in-situ shipping and aircraft emissions. This investigated further via an additional experiment in Sect. 4.3. These two populations cause the correlation to be much lower and also give a larger gradient.

In summary, there is a high correlation between GOME data and TOMCAT results for regions with high NO_2 columns but the model results tend to have higher concentrations in these areas than the data. Over oceans the correlation between the model and GOME data is lower and the GOME columns are higher than the model predicts.

4.3. Long range transport of NO_y

Nitrogen oxides are among the compounds which are controlled by the UNECE Convention on Long-range Trans-boundary Air Pollution and so measurements and the validation of models of global transport of nitrogen oxides are highly important. As a precursor to tropospheric ozone formation long range transport of NO_x is also key to understanding the global budget of ozone. Actual NO_x levels depend on changing sources and sinks along air mass trajectories. For example, in the upper troposphere, NO_x concentrations can be enhanced by in situ emissions (e.g. lightning) or injection of polluted air masses from the surface or by chemical processes such as photolysis of HNO_3 which recycle NO_x from reservoir species.

The source regions considered here are North America where anthropogenic emissions are carried eastwards over the Atlantic, and the westward transport of African biomass burning emissions. It would be useful to be able to examine the fate of Eu-

ropean emissions but this is complicated by the fact that they are not carried over an oceanic region by prevailing winds and so further NO_x emissions occurring downwind complicate any examination of outflow from this region. In addition, in winter when the plumes are most obvious, the region to the east of Europe is very cloudy and there is little or no GOME data for the region downwind of Western Europe in these months.

4.3.1. Export from North America into the Atlantic

Figure 7 appears to show the influence of plumes of NO_2 on the North Atlantic region. For all the months shown we can see a band of elevated concentrations which stretches in a generally northeastward direction from the east coast of the US towards Europe. However this also coincides with a region of both high shipping and aircraft emissions so it is not possible to assign this region of elevated concentrations solely to export.

In January (Fig. 1) the concentrations in this region are higher in TOMCAT than those indicated by the satellite results. This is not a result of different source strengths alone as the NO_2 concentrations over the east coast of the USA are approximately the same in both sets of data. This contrast between the model and satellite data is not however consistent between months. For example in September (Fig. 3) it can be seen that the total column of NO_2 over the North Atlantic in the satellite data is similar to that of the model. In July (Fig. 2) if anything the model is slightly lower than the GOME data. In both July and September the modelled concentrations over the east coast of the US are too high so the agreement over the Atlantic again suggests that there is a problem with the way this export is modelled. It should also be noted that higher NO_2 columns to the east of Europe in the model than in the GOME observations can also be observed.

There are a large number of processes occurring in this region which can have an impact on the concentrations of NO_2. Various studies have shown that warm conveyor belts associated with frontal systems are an important mechanism for transporting emissions from the north east of north America out across the Atlantic. For more details of these flows see Stohl (2001). NO_2 also has a secondary source from HNO_3

and PAN as well as in situ production from lightning and emissions from ships and aircraft.

In order to examine the possibility that the NO_2 in this region is primarily a result of in situ emissions (either anthropogenic or lightning) the model was rerun without any anthropogenic emissions of NO_x from North America. Figure 8 shows the results of this experiment for January. When there are no North American emissions, the high concentrations in the North Atlantic are absent. The high model concentrations in this region cannot be attributed to in situ emissions.

4.3.2. Export from Africa by easterly winds

High NO_2 columns from Africa can be seen off the coast of Africa in the region of easterly winds. In the GOME data in January this transport can be seen from west Africa into the Atlantic but in the TOMCAT data this plume ends very close to the coast, similar to what is seen for July in the modelled Asian plume. However unlike in the mid-latitude plumes the model consistently underestimates the concentrations whether they start from West Africa (in January) or from Central Africa (in July and September). The model's inability to correctly reproduce this export may be part of the reason why the correlation in the South Atlantic has such a low gradient.

One explanation which must be considered is that these elevated columns are not primarily the result of plumes of biomass burning emissions but are from NO_x production by lightning. However, the columns off the coast do seem to be consistent with the elevated concentrations over regions with high biomass burning emissions. The most clear example of this in the GOME data is September when the highest columns are seen over central Africa and the largest columns over the west coast of central Africa are also seen. The seasonal signal of lightning flash frequency is the reverse of that for biomass burning (see for example Jourdain and Hauglustaine, 2001) with a high flash frequency over west Africa in July and higher in southern and central Africa in January and so it seems unlikely that lightning can explain these features. However, some of

the elevated concentrations in July over west Africa may be attributed to lightning.

4.4. Biomass burning distribution and seasonal cycle

In order to examine how well the model captures seasonal variations in biomass burning emissions, it is useful to consider a smaller area than in the previous correlations. Central Africa (9.8–29.5° longitude, 0 to −19.5° latitude) was chosen, because Figs. 1, 2 and 3 show that the seasonal changes are strongest in this region. The seasonal cycle is shown in Fig. 9.

The model agrees very well with the GOME data for the majority of months and the general timing and amplitude of the seasonal cycle are approximately correct especially when the large variability in this area in both the model and the measurements is taken into account. However, the peak in modelled NO_2 concentrations is somewhat earlier and more intense when compared to the peak concentrations in GOME. TOMCAT's peak concentrations are in July and are greater than in the peak in GOME data which occurs in August. The elevated concentrations in GOME persist until October while the TOMCAT columns fall off more quickly. The variability of TOMCAT data in this region is also larger than the variability of the measurements during this peak, whereas earlier in the year it is smaller than observed. Law et al. (2000) have shown using ozone measurements from the MOZAIC program in the upper troposphere over central Africa that TOMCAT and several other CTMs do not exactly capture the seasonal cycle of biomass burning emissions in this region. If a emission inventory based on fire count data for 1997 were to be used in the model it might be expected that the model agreement with GOME and MOZAIC data would improve.

5. Discussion

Clearly, a single model deficiency cannot explain all of the features discussed above. In fact, each of the model discrepancies may be a result of several limitations acting

together. It is therefore useful to consider each of the processes affecting the concentrations and distribution of NO_2 in turn and the limitations in modelling these processes which could lead to such differences.

5.1. GOME retrieval errors

As with all remote sensing measurements, the retrieval of NO_2 columns from GOME is based on a number of a priori assumptions that can introduce errors in the final product. The main uncertainties are related to the vertical distribution of the NO_2, the impact of aerosols, and clouds.

By using vertical profiles from the TOMCAT model run in the data analysis, the retrieval is self-consistent (but not necessarily correct) and any such errors introduced by incorrect TOMCAT profiles are properly discussed under the sections on model errors.

Aerosols have been taken into account in the retrieval in a rather general manner, with only 3 different aerosol scenarios (maritime, rural and urban). Clearly in regions of intense biomass burning visibility can be much reduced, affecting the data but this is not yet accounted for in the analysis. Therefore, the GOME NO_2 columns retrieved for such conditions will tend to underestimate the atmospheric NO_2 content.

Clouds have been treated by rejecting measurements above a threshold value of roughly 10%, thereby reducing the impact of clouds on the retrieval. However, as discussed in several papers (Velders et al., 2001; Richter and Burrows, 2001; Martin et al., 2002) even relatively small cloud fractions can have a significant effect on the result, leading to underestimations of up to 40%, in particular in industrialised regions in winter. Clouds can also lead to an overestimation of NO_2 columns if a significant amount of NO_2 is located above a low cloud layer.

By applying a cloud screening, there also is a systematic bias in the measurements excluding certain atmospheric situations. For example, transport of pollutants is often linked to frontal systems, which are associated with cloud formation and these will be excluded from the GOME data set. This could explain part of the observed difference between model and measurement with respect to export of NO_2 from the US and

Europe, as GOME might systematically be unable to observe such events because of enhanced cloudiness. It might also help explain some of the differences between model performance for Europe and the US. Cloudiness is likely to be a greater problem for Europe than over the whole of North America.

5.2. Emissions

As the major source of NO_x is from surface emissions they play a key role in determining the modelled concentrations. The good correlations and gradients close to 1 for the winter months in polluted regions suggests that the emission inventories are unlikely to be the major source of GOME-TOMCAT differences. However, in terms of the seasonal cycle of differences over Europe, North America and Asia, the lack of a seasonal cycle in the emission inventory used for industrial emissions may play a role. Industrial NO_x emissions are lower in the summer as a result in particular of lower energy requirements for space heating and lighting. However, in the Northern Hemisphere regional emissions only vary by up to 15% from a uniform distribution (Olivier et al., 2003) and so seem unlikely as the major explanation for the differences in the modelled and observed seasonal cycle of NO_2 columns. Also of possible importance are daily cycles of emissions, especially the potential importance of rush hour peaks in NO_x emissions. At higher model resolutions these cycles will probably increase in importance as there will be less model-induced "smearing" of emissions.

Overestimated emissions from polluted regions could explain the large overprediction of model columns over Europe and other polluted regions but there is no other evidence to suggest that the emission inventories could have such a large error. Given that for this inventory industrial emissions were scaled to be appropriate for 1997, trends in emissions are unlikely to have played a significant role in differences between TOMCAT and GOME results.

It is not surprising that the model is unable to resolve the exact timing and intensity of biomass burning in central Africa. This is because the biomass burning inventory used was not specific to 1997 but was based on a climatology. 1997 was a year

in which there was a strong El Niño which caused major changes to the pattern of fires globally. See for example Novelli et al. (2003) and Duncan et al. (2003) and references therein. An inventory based, e.g. on fire count data (or other methods giving more accurate information on the location of fires) is likely to improve the agreement in biomass burning regions.

5.3. Physical processes

The major physical processes which play a role in the distribution of NO_2 are large scale horizontal transport, dry deposition and vertical mixing.

5.3.1. Horizontal transport

One plausible explanation for the model failing to reproduce the observed export of NO_2 from Africa into the Atlantic is that this circulation is not correctly represented in the model. With a half life of 5.5 days and a source which is dominated by terrestrial sources, radon is a very good tracer for considering this question. Figure 10 shows the total column of radon for September 1997. The westward transport of air from West Africa can be clearly seen in this figure and, although not as strong, advection of air from Central Africa over the Atlantic is also visible. This suggests that an incorrectly modelled westward advection is not a major reason why elevated NO_2 columns are not observed in this region in the model results. To test in more detail how well the advection in this region is modelled would require profiles of radon or another short-lived tracer to be measured in this region.

5.3.2. Vertical mixing

When considering the effect of vertical mixing in the model it is important to note that the model profile of NO_2 affects the GOME retrieval. This is because the Air Mass Factor used to convert from slant column data to vertical columns is calculated based on an a-priori NO_2 profile from TOMCAT. The effect of increased vertical mixing either in the

boundary layer or due to stronger convection would decrease the fraction of modelled NO_2 close to the ground thus meaning that the NO_2 column retrieved from the GOME observations would be decreased. Increased vertical mixing in the model would also increase the total modelled column as the lifetime of NO_2 is less at low level. Increased vertical mixing in the model therefore decreases the GOME columns and increases the modelled columns. This implies that GOME-TOMCAT comparisons are especially sensitive to errors in the modelled vertical transport and so are potentially a rigorous test of the model. Convection and boundary layer mixing are very variable in time and space. This means that this study, which uses monthly mean data, is limited in its ability to evaluate in detail these issues. The vertical mixing in a previous version of the TOMCAT model was tested in Stockwell et al. (1998) by comparison with observed profiles of radon. That model version used a local vertical mixing scheme (Louis, 1979) and there was insufficient vertical mixing near the surface. The boundary layer mixing in the model has since been improved by the use of a non-local scheme (Holtslag and Boville, 1993) as documented in Wang et al. (1999). The model now shows much better agreement with the profiles discussed in Stockwell et al. (1998). The boundary layer mixing gives concentrations near the surface which are much closer to the observations.

If the summertime convection over Europe were too strong in the model this would explain the overestimation by TOMCAT of the NO_2 columns. A comparison of TOMCAT profiles with aircraft observations over central Europe in the EXPORT campaign (e.g. O' Connor et al., 2004) seems to indicate that the modelled boundary layer concentrations of NO_2 are too low (probably because the model is unable to resolve local sources) and concentrations in the free troposphere are approximately correct. Brunner et al. (2003) found that for most parts of the free troposphere TOMCAT had a negative bias for NO_x when compared to the results of aircraft observations. This makes it difficult to come to any clear conclusions on whether vertical mixing is the major process causing model-GOME differences.

If the modelled convection over tropical oceans is too weak in the model this might explain the lower NO_2 columns calculated off the coast of West Africa compared to

GOME results. Too little convective activity over oceans in the model might also provide an explanation for the low gradients (mean of 0.31) observed over the south Atlantic. However there is some evidence that the convection over land as modelled in TOMCAT is too weak while that over the oceans is too strong. This again suggests that incorrect vertical mixing does not explain the differences between modelled and satellite NO_2 columns. The modelled export of emissions from source regions would also be underestimated if convective processes over land in the model were to be too weak. Too little convection would cause less of the NO_2 to reach high levels where more rapid horizontal transport occurs and where the NO_x lifetime is longer. If export from polluted regions is too weak in TOMCAT, due to weak convection over the land this would partially explain the low concentrations off the west coast off Africa.

The question of vertical mixing in chemistry-transport models is one which deserves further work and this would best be addressed by an approach which combined satellite and aircraft measurements in a series of well chosen case studies.

5.3.3. Dry deposition

NO_2 is dry deposited at the surface. The deposition velocity is not large so this is unlikely to be a cause of model-measurement differences. Nevertheless, if the dry deposition in the model is too strong it could affect both the modelled NO_2 column and the retrieval. Increasing dry deposition would reduce the total modelled column but it would also change the vertical profile of NO_2. A smaller fraction of the NO_2 near the surface would change the Air Mass Factor calculated from the model data and so reduce the column density in the GOME retrieval because the retrieval is less sensitive to NO_2 at lower levels. Unlike for changes in vertical transport therefore the satellite-model comparison is relatively insensitive to errors in the modelled dry deposition.

5.4. Chemistry

The two main limitations in the model chemistry scheme which might explain the differences between the model and GOME data are the limited number of hydrocarbons in the model and, in particular, the absence of isoprene chemistry. These enhancements of the model chemistry would favour rapid formation of PAN and higher homologues in the boundary layer. This could result in lower NO_2 concentrations over polluted areas as well as higher columns in regions where the air is descending when NO_2 is subsequently released due to thermal decomposition. Any other missing gas phase or multiphase reactions of oxides of nitrogen would be a part explanation of the differences between model and GOME NO_2. It is quite likely that there are different weaknesses in the model chemistry scheme in the marine boundary layer, the polluted boundary layer and the free troposphere.

5.5. Model resolution

The low resolution of the model will cause rapid mixing of emissions and so tend to reduce the concentrations of the highest peaks and increase the concentrations over the more remote regions. However it is not clear from the correlation plots that this is a major issue The model uses an advection scheme which preserves gradients reasonably well. In addition in regions of high emissions, NO may remove most of the ozone, thus creating a high NO/NO_2 ratio. This would not be observed in the model results if regions of high emissions are smeared out in the model. This could lead to the model having too much NO_2 and might help explain the larger NO_2 columns in the model over polluted areas.

5.6. Cloud effects on model results

In the GOME retrieval used for this study cloudy pixels are not used to calculate the tropospheric NO_2 column. This introduces an inconsistency between the model and

ACPD
4, 2569–2613, 2004

measurements. In TOMCAT photolysis rates in the model are calculated using latitudinally averaged cloud climatologies. This means that the photolysis rates of NO_2 in the model are lower than those in the real atmosphere where the GOME measurements are made (as only cloud free pixels are included). It might be expected that this lower modelled photolysis rate would lead to a higher NO_2/NO_x ratio in the model thus potentially explaining part of the positive bias of the modelled values over polluted regions. However, this cannot explain the difference in seasonality between TOMCAT and GOME over polluted regions. As the cloudiness is greatest in winter this would imply that the model should have a stronger positive bias in the winter months whereas in fact this is when the best agreement is found. An estimate of the order of magnitude of this effect can be found by taking the ratio of photolysis rates calculated for cloudy to non-cloudy scenarios. For a latitude of 53° N in June this ratio is 0.82. This means that this is potentially a significant effect but cannot alone explain the model-GOME differences.

To remove this bias from the model would require 2 changes to the methods used here. Firstly a photolysis scheme coupled to cloudiness data input from the meteorological analyses would have to be included in the model. In addition, it would be necessary to sample the model at the time and place of each GOME measurement used to calculate the monthly mean instead of using the monthly mean column at 10:30 local time. This would be a valuable case study to perform in the future.

6. Conclusions

The successful modelling of tropospheric NO_x is a major challenge for CTMs (e.g. Brunner et al., 2003). Given that, the TOMCAT model is overall in reasonably good agreement with the GOME data but has a positive bias with a correlation coefficient of 0.79 and a gradient of 1.5 for the whole world. The best agreement with the GOME data is in Africa for most months of the year and in the polluted Northern Hemisphere in winter. However three main areas of disagreement have been found: the seasonal

cycle of NO_2 columns over polluted areas, regions of pollution export over oceans and the exact distribution and intensity of biomass burning distributions. Future model development activities should consider GOME NO_2 data as a highly important set data for testing any changes made to models and new emission inventories. The most important explanations for disagreements between the model and measurements seem likely to be limitations in the model chemistry scheme and limitations in the vertical transport schemes (convection and boundary layer).

Possible methods for improving the performance of the TOMCAT model include: including seasonal cycles in anthropogenic emissions; better treatment of clouds; additional NMHC chemistry, especially that of isoprene, and a parameterisation for N_2O_5 loss on aerosol. Also the use of multi-annual model runs will allow the variability of these model-GOME differences to be considered which will hopefully also provide further insight into the atmospheric chemistry of NO_2 in both the model and the real atmosphere. Higher resolution simulations with TOMCAT would allow the effect of model resolution to be examined. A new parallel version of the model has been developed and this will allow additional chemistry and other model improvements in the future. Finally, case studies of specific events such as Warm Conveyor Belts (Stohl, 2001) or a "meteorological bomb" (Stohl et al., 2003) could provide valuable insight into how well transport pathways from polluted areas are modelled. Other case studies should concentrate on periods where there is satellite data coincident with an aircraft campaign. To investigate the effects of cloudiness on the GOME-model comparison would require an on-line photolysis scheme in the model and the sampling of the model at the time and place of each GOME measurement rather than simply using data output at 10:30 local time.

Acknowledgements. This work was carried out as part of the European Union funded program POET (ENVK2-CT1999-00011) and was funded in part by the University of Bremen, German Aerospace Agency (DLR) and the German Ministry for Education and Research (BMBF). The authors would like to thank M. Chipperfield for providing SLIMCAT model data and R. Koelemeijer for making the surface reflectivity data base available. The authors would like to thank F. O'Connor for her advice and comments on the text. We also acknowledge the ECMWF

for allowing access to their meteorological analyses and the British Atmospheric Data Centre (BADC) for supplying them. The authors also acknowledge NCAR for supplying the planetary boundary layer scheme from their Community Climate Model (CCM2).

References

Borrell, P., Builtjes, P., Genfelt, P., and Hov, Ø.: Photo-Oxidants, Acidification and Tools: Policy Applications of Eurotrac Results, Springer-Verlag Berlin Heidelberg, ISBN 3-540-61783-3, 1997. 2571

Brunner, D., Staehelin, J., Rogers, H. L., Köhler, M. O., Pyle, J. A., Hauglustaine, D., Jourdain, L., Berntsen, T. K., Gauss, M., Isaksen, I. S. A., Meijer, E., van Velthoven, P., Pitari, G., Mancini, E., Grewe, V., and Sausen, R.: An evaluation of the performance of chemistry transport models by comparison with research aircraft observations, Part 1: Concepts and overall model performance, Atm. Chem. Phys., 3, 1609–1631, 2003. 2571, 2590, 2593

Burkert, J., Andres-Hernandez, M. D., Stobener, D., Burrows, J. P., Weissenmayer, M., and Kraus, A.: Peroxy radical and related trace gas measurements in the boundary layer above the Atlantic Ocean, J. Geophys. Res., 106, D6, 5457–5477, 2001. 2580

Burrows, J. P., Weber, M., Buchwitz, M., Rozanov, V., Ladstätter-Weißenmayer, A., Richter, A., DeBeek, R., Hoogen, R., Bramstedt, K., Eichmann, K.-U., Eisinger, M., and Perner, D.: The Global Ozone Monitoring Experiment (GOME): Mission Concept and First Scientific Results, J. Atmos. Sci., 56, 151–175, 1999. 2573

Carver, G. D., Brown, P. D., and Wild, O.: The ASAD atmospheric chemistry integration package and chemical reaction database, Comput. Phys. Commun., 105, (2–3), 197–215, 1997. 2576

Chameides, W. L., Fehsenfeld, F., Rodgers, M. O., Cardelino, C., Martinez, J., Parrish, D., Lonneman, W., Lawson, D. R., Rasmussen, R. A., Zimmerman, P., Greenberg, J., Middleton, P., and Wang, T.: Ozone Precursor Relationships in the Ambient Atmosphere, J. Geophys. Res., 97, D5, 6037–6055, 1992. 2570

Chipperfield, M. P.: Multiannual Simulations with a Three-Dimensional Chemical Transport Model, J. Geophys. Res., 104, 1781–1805, 1999. 2574

Duncan, B. N., Bey, I., Chin, M., Mickley, L. J., Fairlie, T. D., Martin, R. V., and Matsueda, H.:

Indonesian wildfires of 1997: Impact on tropospheric chemistry, J. Geophys. Res., 108, D15, 4458, 2003. 2589
ESA (European Space Agency): GOME Global Ozone Monitoring Experiment users manual, ESA SP-1182, ESA/ESTEC, Noord-wijk, Netherlands, ISBN 92-9092-327-x, 1995. 2574
Eskes, H. J. and Boersma, K. F.: Averaging kernels for DOAS total-column satellite retrievals, Atmos. Chem. Phys., 3, 1285–1291, 2003. 2575
Fishman, J. and Crutzen, P.: The origin of ozone in the troposphere, Nature, 274, 855–858, 1978.
Grewe, V., Brunner, D., Dameris, M., Grenfell, J. L., Hein, R., Shindell, D., and Staehelin, J.: Origin and variability of upper tropospheric nitrogen oxides and ozone at northern mid-latitudes, Atm. Env., 35, 20, 3421–3433, 2001. 2571
Haagen-Smit, J. A.: Chemistry and physiology of Los Angles smog. Ind. Eng. Chem., 44, 1342–1346, 1952. 2570
Hao, W. M. and Liu, M. H.: Spatial and Temporal distribution of tropical biomass burning, Global Bigechem. Cyc., 8, (4), 495–503, 1994. 2580
Harris, G. W., Klemp, D., Zenker, T., Burrows, J. P., and Mathieu B.: Tunable diode-laser measurements of trace gases during the 1988 POLARSTERN cruise and intercomparisons with other methods, J. Atm. Chem., 15, 3–4, 315–326, 1992. 2580
Holtslag, A. A. M. and Boville, B. A.: Local versus nonlocal boundary layer diffusion in a global climate model, J. Clim., 6, (10), 1825–1842, 1993. 2576, 2590
Houghton, J. T., Ding, Y., Griggs, D. J., Noguer, M., van der Linden, P. J., and Xiaosu, D. (Eds.): Climate Change 2001: The Scientific Basis Contribution of Working Group I to the Third Assessment Report of the Intergovernmental Panel on Climate Change (IPCC), Cambridge University Press, UK, 2001. 2570
Isobe, T., Feigelson, E. D., Akritas, M. G., and Babu, G. J.: Linear Regression in Astronomy, I. Astrophysical J., 105, (2–3), 197–215, 1997. 2578
Jacob, D. J., Prather, M. J., Rasch, P. J., Shia, R. L., Balkanski, Y. J., Beagley, S. R., Bergmann, D. J., Blackshear, W. T., Brown, M., Chiba, M., Chipperfield, M. P., deGrandpré, J., Dignon, J. E., Feichter, J., Genthon, C., Grose, W. L., Kasibhatla, P. S., Köhler, I., Kritz, M. A., Law, K., Penner, J. E., Ramonet, M., Reeves, C. E., Rotman, D. A., Stockwell, D. Z., Van Velthoven, P. F. J., Verver, G., Wild, O., Yang, H., and Zimmermann, P.: Evaluation and intercomparison of global atmospheric transport models using Rn-222 and other short-lived tracers, J. Geophys. Res., 102, (D5), 5953–5970, 1997. 2577

Jourdain, L. and Hauglustaine, D. A.: The global distribution of lightning NO_x simulated on-line in a general circulation model, Phys. Chem. Earth., 26, C8, 585–591, 2001. 2585
Koelemeijer, R. B. A., Stammes, P., Hovenier, J. W., and de Haan, J. F.: A fast method for retrieval of cloud parameters using oxygen, A band measurements from the Global Ozone Monitoring Experiment, J. Geophys. Res., 106, 3475–3490, 2001. 2575
Kunhikrishnan, T., Lawrence, M. G., von Kuhlmann, R., Richter, A., Ladstätter-Weißenmayer, A., and Burrows, J. P.: Analysis of tropospheric NOx over Asia using the model of atmospheric transport and chemistry (MATCH-MPIC) and GOME-satellite observations, Atm. Env., 38, 4, 581–596, 2004. 2572, 2582
Landsman, W. B.: Astronomical Data Analysis Software and Systems II, A. S. P. Conference Series, 52, p. 246, 1993. 2578
Lauer, A., Dameris, M., Richter, A., and Burrows, J. P.: Tropospheric NO2 columns: a comparison between model and retrieved data from GOME measurements, Atm. Chem. Phys., 2, 67–78, 2002. 2572, 2579, 2582
Law, K. S., Plantevin, P. H., Shallcross, D. E., Rogers, H. L., Pyle, J. A., Grouhel, C., Thouret, V., and Marenco A.: Evaluation of modeled O_3 using Measurement of Ozone by Airbus In-Service Aircraft (MOZAIC) data, J. Geophys. Res., 103, (D19), 25 721–25 737, 1998.
Law, K. S., Plantevin, P. H., Thouret, V., Marenco, A., Asman, W. A. H., Lawrence, M., Crutzen, P. J., Muller, J. F., Hauglustaine, D. A., and Kanakidou, M.: Comparison between global chemistry transport model results and Measurement of Ozone and Water Vapor by Airbus In-Service Aircraft (MOZAIC) data, J. Geophys. Res., 105, D1, 1503–1525, 2000. 2586
Leue, C., Wenig, M., Wagner, T., Platt, U., and Jähne, B.: Quantitative analysis of NO_x emissions from GOME satellite image sequences, J. Geophys. Res., 106, 5493–5505, 2001.
Louis, J. F.: A parametric model of vertical eddy fluxes on the atmosphere, Boundary Layer Meteorol., 17, 187–202, 1979. 2590
Martin, R. V., Chance, K., Jacob, D. J., Kurosu, T. P., Spurr, R. J. D., Bucsela, E., Gleason, J. F., Palmer, P. I., Bey, I., Fiore, A. M., Li, Q. B., Yantosca, R. M., and Koelemeijer, R. B. A.: An improved retrieval of tropospheric nitrogen dioxide from GOME, J. Geophys. Res., 107, D20, 4437, 2002. 2573, 2578, 2580, 2581, 2587
Novelli, P. C., Masarie, K. A., Lang, P. M., Hall, B. D., Myers, R. C., and Elkins, J. W.: Reanalysis of tropospheric CO trends: Effects of the 1997–1998 wildfires, J. Geophys. Res., 108, D15, 4464, 2003. 2589
O'Connor, F. M., Law, K. S., Pyle, J. A., Barjat, H., Brough, N., Dewey, K., Green, T., Kent,

J., and Phillips, G.: Tropospheric Ozone Budget: Regional and Global Calculations, Atmos. Chem. Phys. Discuss., 4, 991–1036, 2004. 2590

Olivier, J. G. J. and Berdowski, J. J. M.: Global emission sources and sinks, "The Climate System", edited by Berdowski, J., Guicherit, R., and Heij, B. J., pp. 33–78, A. A. Balkema Publishers/Swets & Zeitlinger Publishers, Lisse, The Netherlands, ISBN 90-5809-255-0, 2001. 2576, 2579

Olivier, J., Peters, J., Granier, C., Petron, G., Müller, J. F., and Wallens, S.: Present and future surface emissions of atmospheric compounds, POET report #2, EU project EVK2-1999-00011, 2003. 2576, 2588

Prather, M. J.: Numerical advection by conservation of second-order moments, J. Geophys. Res., 91, 6671–6681, 1986. 2576

Rasch, P. J., Feichter, J., Law, K., Mahowald, N., Penner, J., Benkovitz, C., Genthon, C., Giannakopoulos, C., Kasibhatla, P., Koch, D., Levy, H., Maki, T., Prather, M., Roberts, D. L., Roelofs, G. J., Stevenson, D., Stockwell, Z., Taguchi, S., Kritz, M., Chipperfield, M., Baldocchi, D., McMurry, P., Barrie, L., Balkansi, Y., Chatfield, R., Kjellstrom, E., Lawrence, M., Lee, H. N., Lelieveld, J., Noone, K. J., Seinfeld, J., Stenchikov, G., Schwartz, S., Walcek, C., and Williamson, D.: A comparison of scavenging and deposition processes in global models: results from the WCRP Cambridge Workshop of 1995, Tellus B 52, (4), 1025–1056, 2000. 2577

Richter, A. and Burrows, J. P.: Tropospheric NO2 from GOME measurements, Adv. Space Res., 29, (11), 1673–1683, 2002. 2574, 2575, 2587

Savage, N. H., Pyle, J., Laq, K., Granier, C., Niemeier, C., Clerbaux, C., Hadji–Lazaro, J., Müller J. F., Dalsøren, S., Isaksen, I., Richter, A., Burrows, J., and Wittrock, F.: Intercomparison of Chemistry-Transport models, POET Report #3, EU project EVK2-1999-00011, 2003. 2576, 2577

Schultz, M. G., Jacob, D. J., Wang, Y., Logan, J. A., Atlas, E. L., Blake, D. R., Blake, N. J., Bradshaw J. D., Browell, E. V., Fenn, M. A., Flocke, F., Gregory, G. L., Heikes, B. G., Sachse, G. W., Sandholm, S. T., Shetter, R. E., Singh, H. B., and Talbot, R. W.: On the origin of tropospheric ozone and NO_x over the tropical South Pacific, J. Geophys. Res., 104, D5, 5829–5843, 1999.

Sillman, S., Logan, J. A., and Wolfsy, S. C.: The sensitivity of ozone to nitrogen oxides and hydrocarbons in regional ozone episodes, J. Geophys. Res., 100, D7, 1837–1851, 1990. 2572

Stockwell, D. Z., Kritz, M. A., Chipperfield, M. P., and Pyle, J. A.: Validation of an off-line three-dimensional chemical transport model using observed radon profiles, 2. Model results, J. Geophys. Res., 103, D7, 8433–8445, 1998. 2590

Stohl, A.: A 1-year Lagrangian "climatology" of airstreams in the Northern Hemisphere troposphere and lowermost stratosphere, J. Geophys. Res., 106, D7, 7263–7279, 2001. 2584, 2594

Stohl, A., Huntrieser, H., Richter, A., Beirle, S., Cooper, O. R., Eckhardt, S., Forster, C., James, P., Spichtinger, N., Wenig, M., Wagner, T., Burrows, J. P., and Platt, U.: Rapid intercontinental air pollution transport associated with a meteorological bomb, Atmos. Chem. Phys., 3, 969–985, 2003. 2594

Thakur, A. N., Singh, H. B., Mariani, P., Chen, Y., Wang, Y., Jacob, D. J., Brasseur, G., Muller, J. F., and Lawrence, M.: Distribution of reactive nitrogen species in the remote free troposphere: data and model comparisons, Atm. Env., 33, 1403–1422, 1999. 2571, 2572

Tiedtke, M.: A comprehensive mass flux scheme for cumulus parameterisation in large-scale models, Mon. Weather Rev., 117, 1779–1800, 1989. 2576

Velders, G. J. M., Granier, C., Portmann, R. W., Pfeilsticker, K., Wenig, M., Wagner, T., Platt, U., Richter, A., and Burrows, J. P.: Global tropospheric NO_2 column distributions: Comparing 3-D model calculations with GOME measurements, J. Geophys. Res., 106, 12 643–12 660, 2001. 2572, 2575, 2579, 2587

Wang, K. Y., Pyle, J. A., Sanderson, M. G., and Bridgeman, C.: Implementation of a convective atmospheric boundary layer scheme in a tropospheric chemistry transport model, J. Geophys. Res., 104, D19, 23 729–23 745, 1999. 2590

World Meteorological Organisation Bulletin, 6, 134–138, 1957. 2578

Table 1. Global correlations using various methods.

	Best Correl	Grad.	Intercept (molec. cm^{-3})	Standard Output Correl	Grad.	Intercept (molec. cm^{-3})	WMO Correl	Grad.	Intercept (molec. cm^{-3})
Mean	0.79	1.47	−0.15E15	0.79	1.89	−0.18E15	0.77	1.5	0.05E15
St Dev	0.04	0.23	0.11E15	0.04	0.27	0.14E15	0.04	0.23	0.12E15

Table 2. Regions used for study.

Region	Longitude (Degrees E)	Latitude (Degrees N)
Africa	343.1–45.0	−36.3–30.7
Asia	39.4–151.9	8.4–72.6
Europe	−11.3–42.2	33.5–72.6
N. America	227.8–281.3	22.3–72.6
N. Atlantic	298.1–340.3	8.4–72.6
S. Atlantic	329.1–360.0	−72.6–0

Table 3. Correlations for Africa, Asia and Europe.

Month	Africa Correlation	Grad.	intercept (molec. cm^{-3})	Asia Correlation	Grad.	intercept (molec. cm^{-3})	Europe Correlation	Grad.	intercept (molec. cm^{-3})
1	0.82	1.23	−0.37E15	0.67	1.09	0.03E15	0.74	0.62	1.69E15
2	0.70	1.16	−0.50E15	0.70	1.40	−0.02E15	0.66	1.47	1.11E15
3	0.79	0.81	−0.15E15	0.75	1.37	−0.19E15	0.84	1.63	0.09E15
4	0.81	0.68	−0.07E15	0.74	1.63	−0.27E15	0.79	1.58	0.96E15
5	0.82	0.82	−0.21E15	0.72	1.86	−0.41E15	0.75	2.62	0.06E15
6	0.65	1.05	−0.12E15	0.78	1.61	0.11E15	0.68	3.14	−1.00E15
7	0.73	1.68	−0.59E15	0.70	1.60	−0.10E15	0.79	2.97	−1.77E15
8	0.73	1.61	−0.63E15	0.72	1.76	−0.27E15	0.90	2.42	−1.11E15
9	0.68	1.41	−0.59E15	0.66	1.79	−0.36E15	0.86	1.86	−0.42E15
10	0.76	0.96	−0.17E15	0.77	1.85	−0.24E15	0.86	1.74	0.21E15
11	0.72	1.77	−0.56E15	0.82	1.45	−0.21E15	0.86	1.51	0.62E15
12	0.86	1.56	−0.03E15	0.54	0.86	0.26E15	0.73	1.20	0.58E15
Mean	0.76	1.23	−0.33E15	0.71	1.52	−0.14E15	0.79	1.90	0.08E15

ACPD
4, 2569–2613, 2004

Table 4. Correlations for North America and North and South Atlantic.

Month	N America Correlation	Grad.	intercept (molec. cm^{-3})	N Atlantic Correlation	Grad.	intercept (molec. cm^{-3})	S Atlantic Correlation	Grad.	intercept (molec. cm^{-3})
1	0.86	0.98	0.17E15	0.38	1.28	0.07E15	0.55	0.47	0.0E15
2	0.83	1.05	0.10E15	−0.04	−0.99	0.36E15	0.34	0.47	−0.1E15
3	0.87	1.33	−0.09E15	0.09	0.94	−0.13E15	0.36	0.55	0.0E15
4	0.93	1.29	−0.07E15	0.01	0.99	−0.06E15	0.47	0.65	0.0E15
5	0.92	1.61	−0.10E15	−0.06	−0.94	0.45E15	0.68	0.38	0.0E15
6	0.93	1.39	−0.12E15	0.40	0.87	−0.07E15	0.48	0.38	0.0E15
7	0.93	1.40	−0.28E15	0.62	0.84	−0.17E15	0.58	0.43	0.0E15
8	0.89	1.74	−0.50E15	0.48	0.87	−0.15E15	0.77	0.31	0.0E15
9	0.93	1.65	−0.32E15	0.58	0.96	−0.10E15	0.53	0.27	0.0E15
10	0.92	1.63	−0.20E15	0.59	1.30	0.03E15	0.58	0.24	0.0E15
11	0.92	1.22	0.06E15	0.50	1.28	0.04E15	0.17	0.47	0.0E15
12	0.79	1.55	−0.10E15	0.67	1.07	0.12E15	−0.01	−0.96	0.0E15
Mean	0.89	1.40	−0.12E15	0.35	0.70	0.03E15	0.46	0.31	−0.05E15

ACPD
4, 2569–2613, 2004

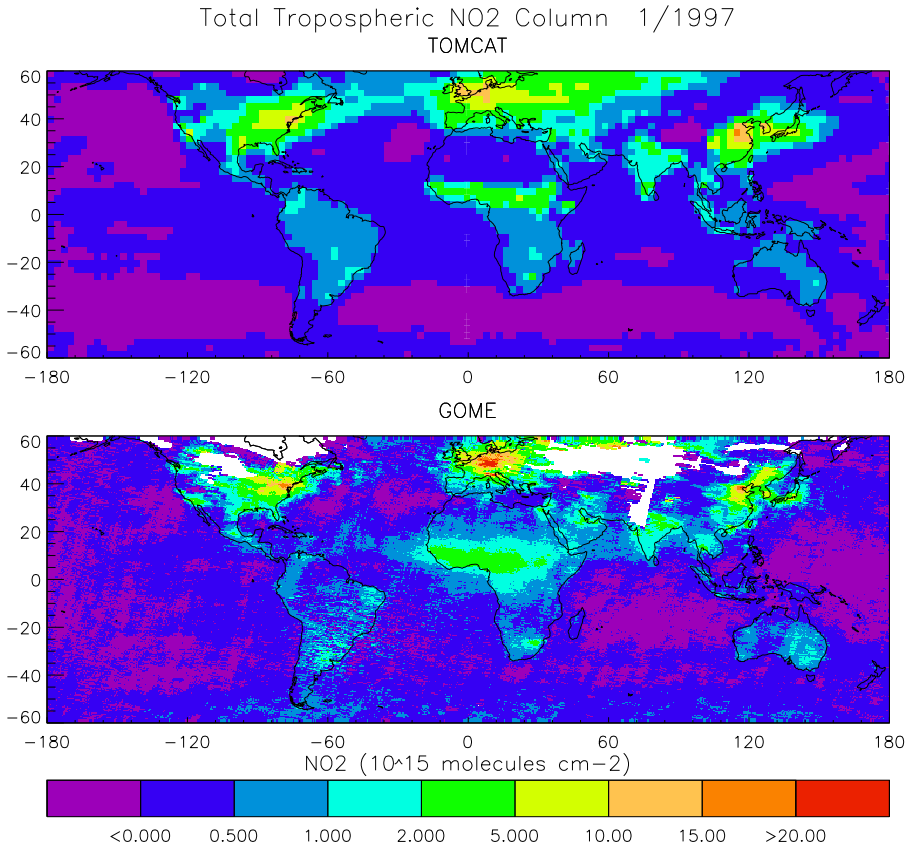

Fig. 1. Monthly mean tropospheric NO_2 columns for January 1997 from the TOMCAT model (top) and the GOME retrieval (below). The TOMCAT results are at the model resolution of 2.8×2.8° while the GOME results have been averaged on to a 0.5×0.5° grid. TOMCAT gives generally good agreement with the satellite data. The highest columns are correctly located and are of the right order of magnitude.

ACPD
4, 2569–2613, 2004

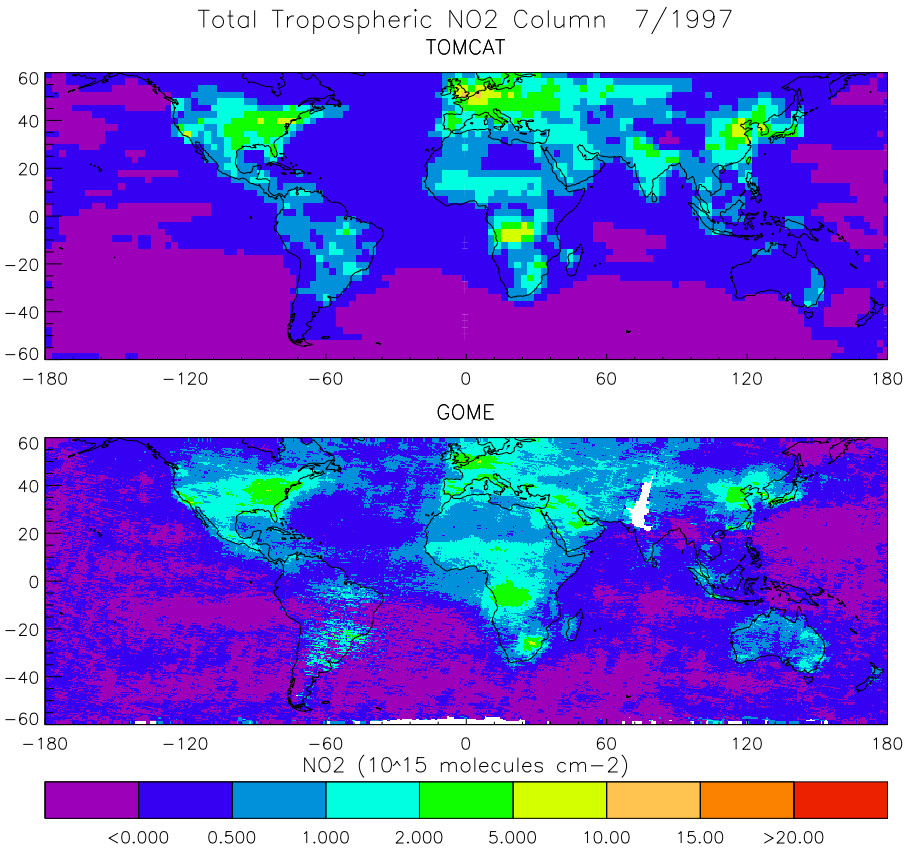

Fig. 2. Monthly mean tropospheric NO_2 columns for July 1997. As for Fig. 1. The overestimation of the NO_2 columns over Europe is quite pronounced and the model also appears to have concentrations which are too great over central Africa also.

ACPD
4, 2569–2613, 2004

TOMCAT CTM versus GOME data

N. H. Savage et al.

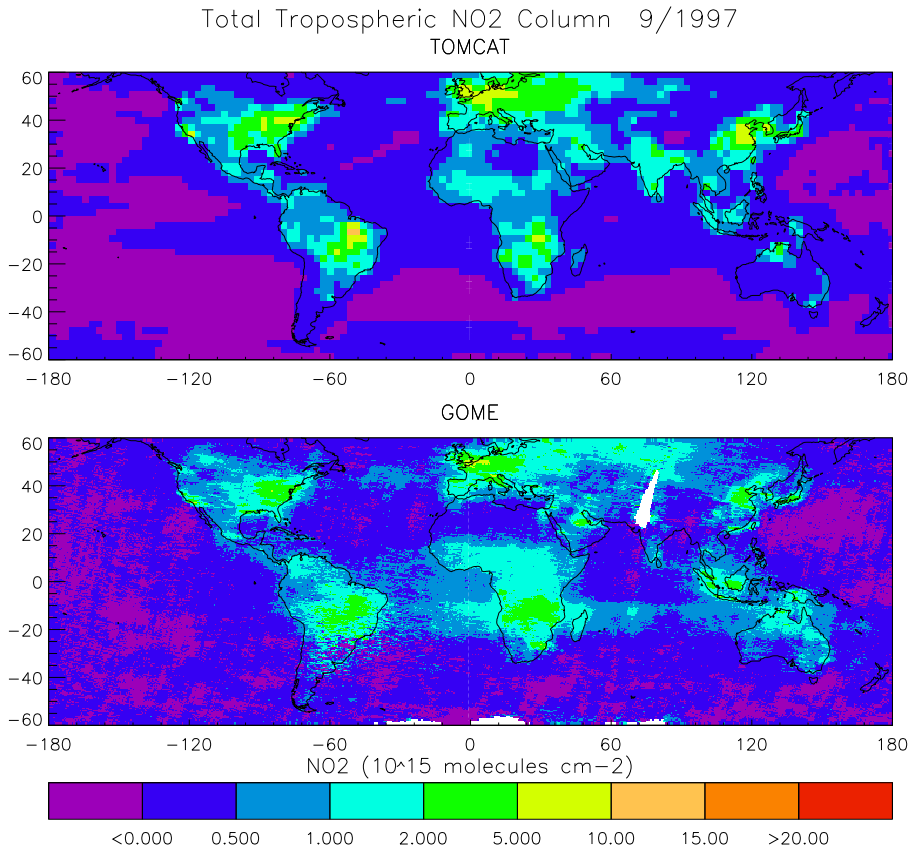

Fig. 3. Monthly mean tropospheric NO_2 columns for September 1997. As for Fig. 1. Note the region of high columns off the west coast of central Africa in the GOME results which may indicate a region of outflow. This is not seen in the TOMCAT results.

ACPD
4, 2569–2613, 2004

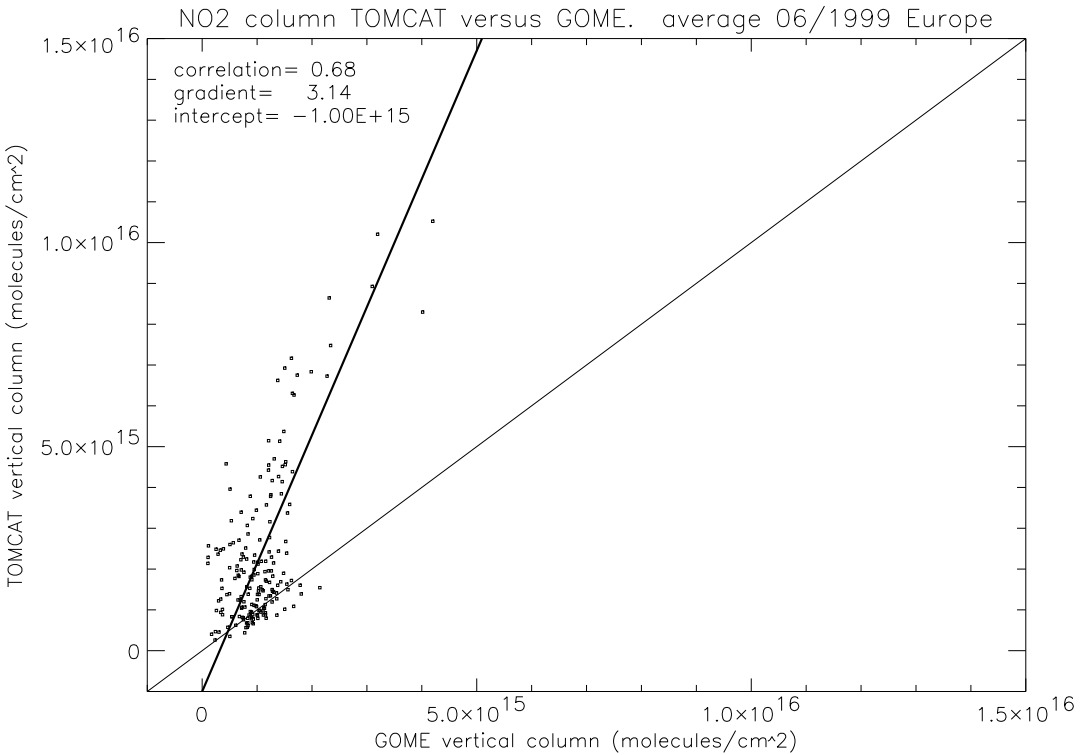

Fig. 4. Scatter plot of tropospheric NO_2 columns TOMCAT results versus GOME retrieval. Europe, June 1997. Thin line 1:1 ratio, thick line least squares fit. Although the TOMCAT results are well correlated with the satellite data, a large fraction of the points are above the 1:1 line and the best fit has a gradient of 3.14.

ACPD
4, 2569–2613, 2004

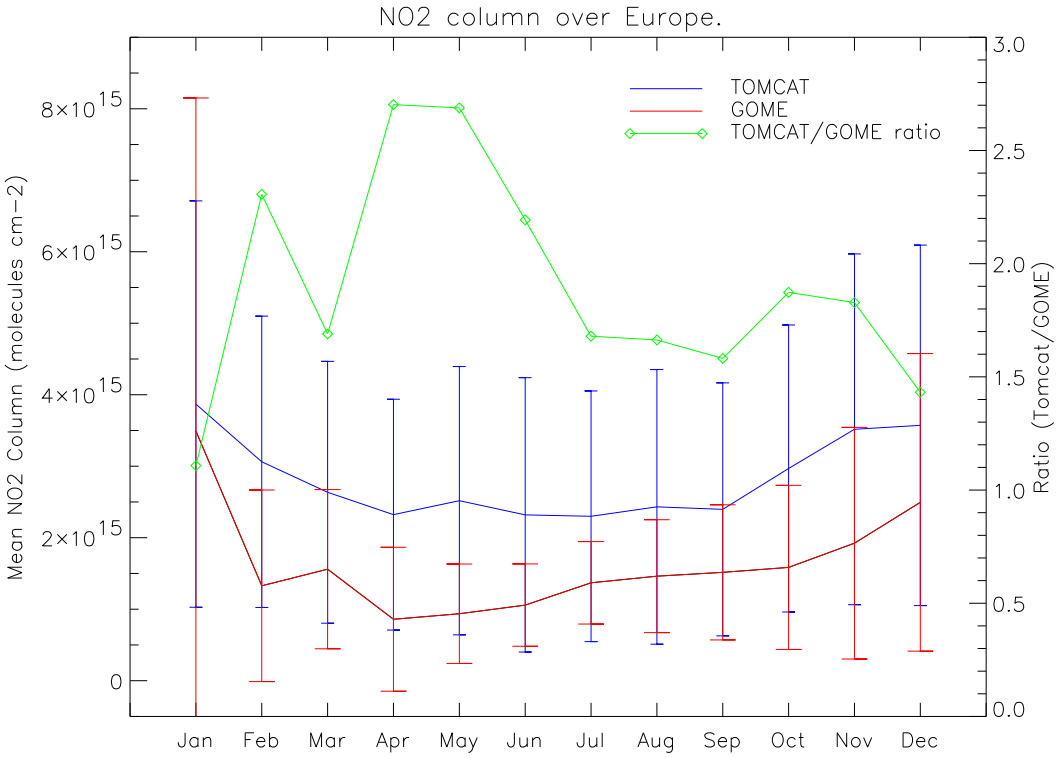

Fig. 5. Seasonal cycle of average tropospheric NO_2 columns over Europe as calculated by TOMCAT (middle line, in blue) and from GOME data (lower line, in red). Error bars indicate the standard deviation of the column over the area. The TOMCAT/GOME ratio is in green. The TOMCAT columns are higher than the GOME values for all months and also decrease less in the summer months compared to winter.

ACPD
4, 2569–2613, 2004

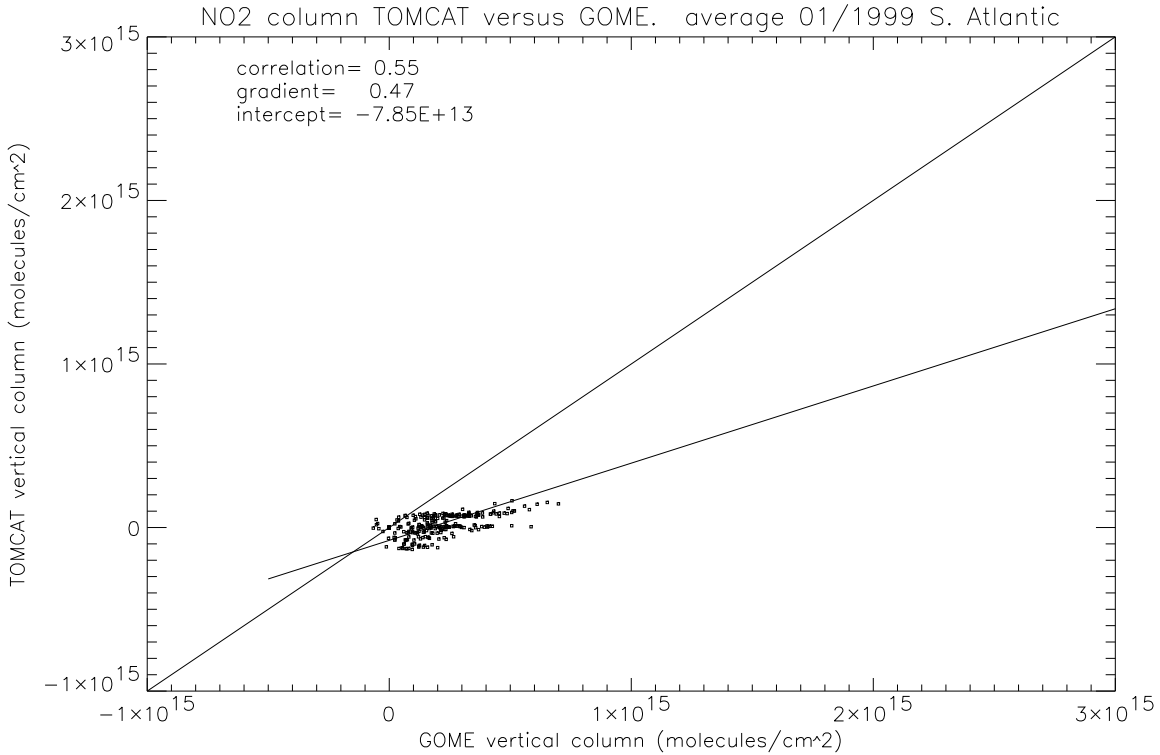

Fig. 6. Scatter plot of tropospheric NO_2 columns TOMCAT results versus GOME retrieval. For South Atlantic January 1997. As Fig. 4. In contrast to the scatter plot for Europe, over the south Atlantic a large proportion of the TOMCAT points are below the 1:1 line.

ACPD
4, 2569–2613, 2004

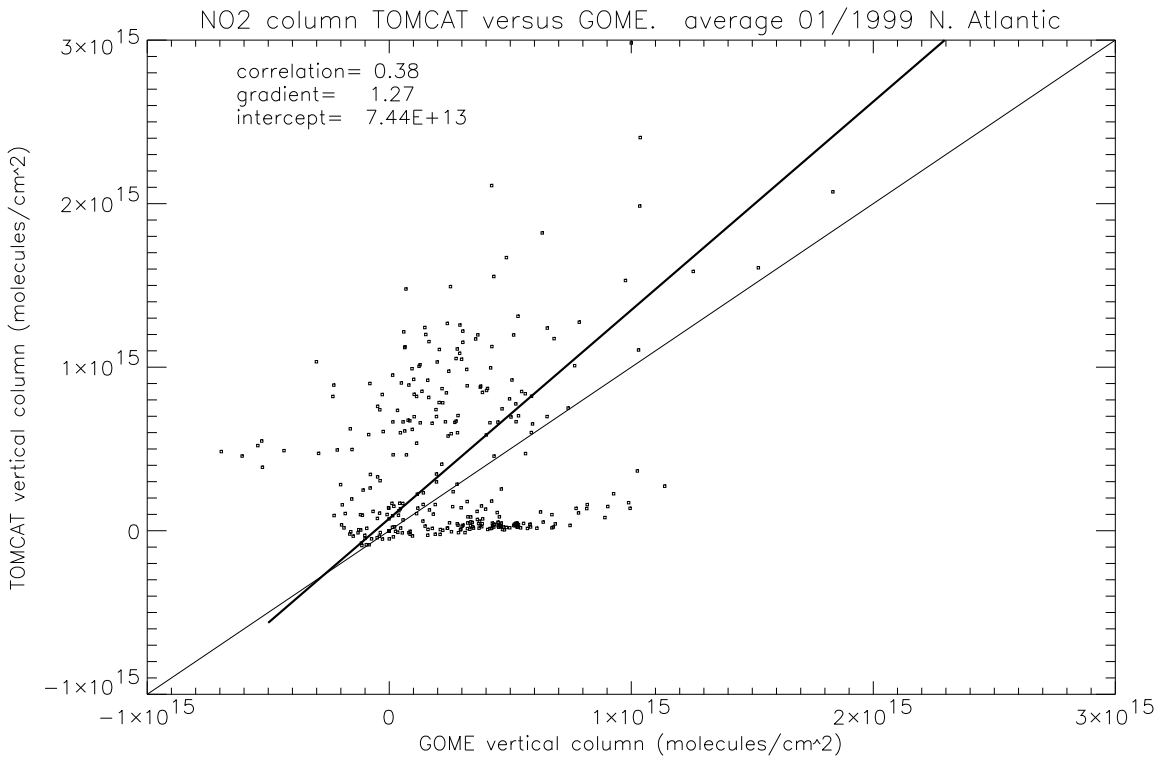

Fig. 7. Scatter plot of tropospheric NO_2 columns TOMCAT results versus GOME retrieval. For North Atlantic January 1997. As Fig. 4. This scatter plot shows how there appear to 2 populations of data in the North Atlantic: one similar to the South Atlantic and another above the 1:1 line which is closer to the European population.

ACPD
4, 2569–2613, 2004

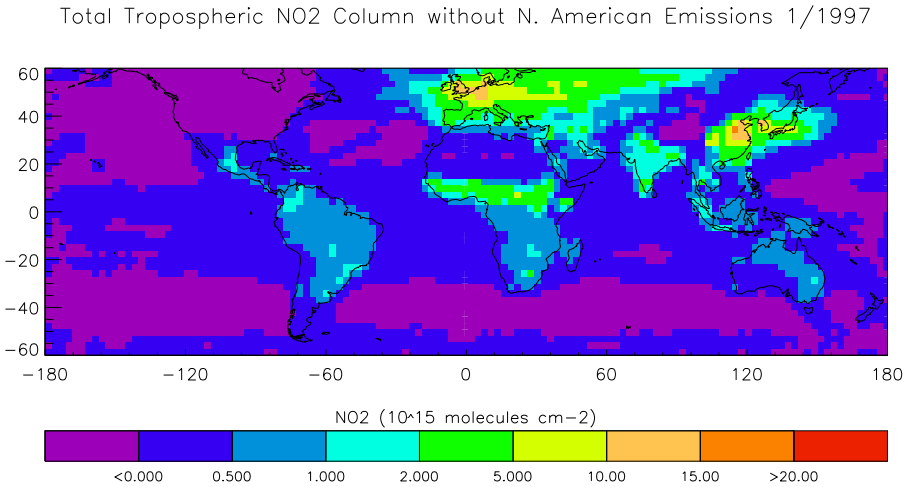

Fig. 8. Tomcat tropospheric NO_2 column for January 1997 without North American Anthropogenic emissions. This shows how without N. American emissions the band starting from the east coast of the USA is not present, giving strong evidence that this feature is due to the export of North American emissions.

ACPD
4, 2569–2613, 2004

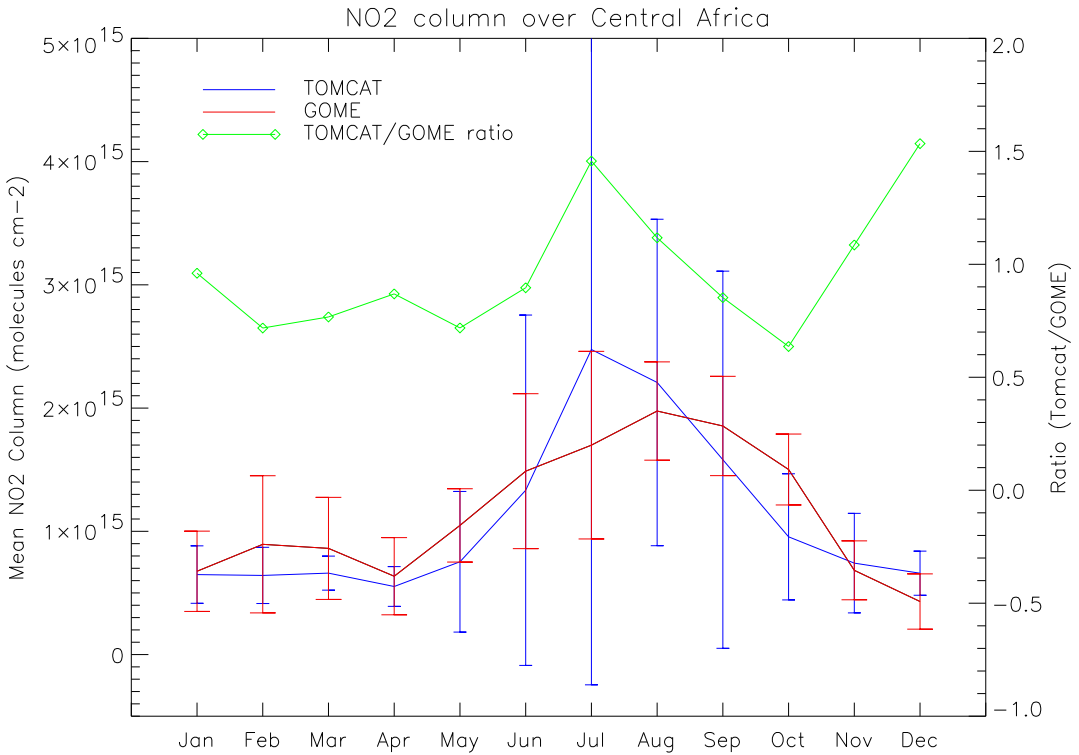

Fig. 9. Seasonal cycle of average tropospheric NO_2 columns over Central Africa as calculated by TOMCAT model (in blue) and from GOME data (in red). Error bars indicate the standard deviation of the column over the area. The TOMCAT/GOME ratio is in green. In comparison to Europe the TOMCAT columns agree much better with the GOME columns. However, the peak in the TOMCAT column is earlier and higher than for GOME. In addition during the period of high columns the standard deviation is much greater for the TOMCAT results than in the GOME data.

ACPD
4, 2569–2613, 2004

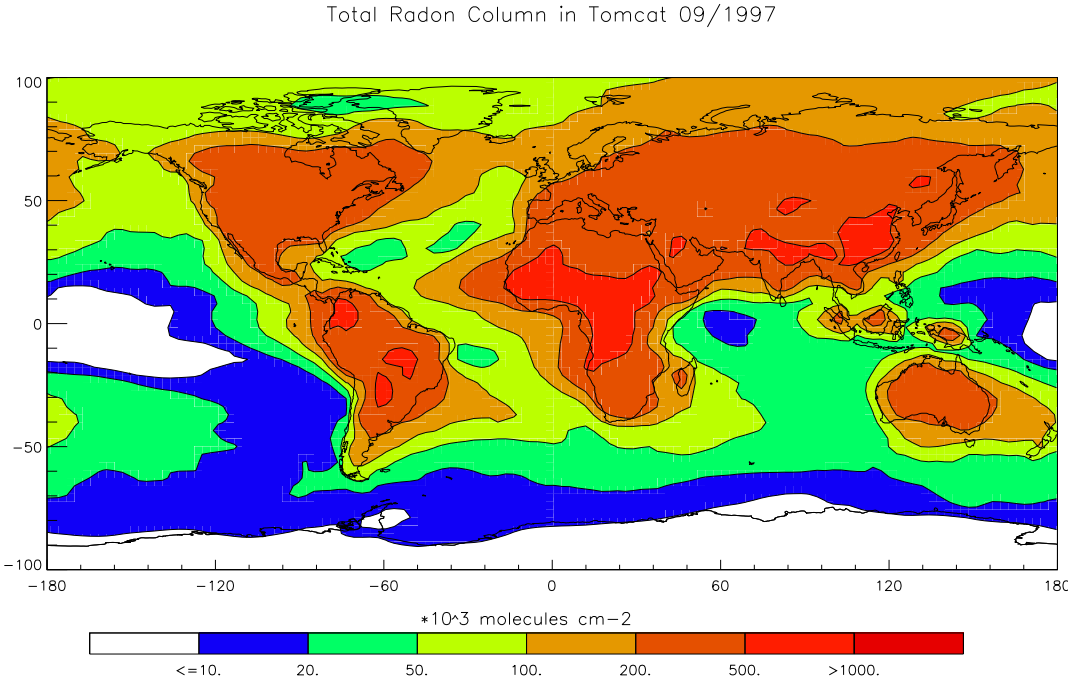

Fig. 10. Total column of Radon from the TOMCAT model September 1997. The regions of outflow from North America, Asia and Africa can all be seen in the radon column.

ACPD

4, 2569–2613, 2004

TOMCAT CTM versus GOME data

N. H. Savage et al.